

Offshore Wind Farm Layout Optimization Using Particle Swarm Optimization

Ajit C. Pillai · John Chick · Lars Johanning ·
Mahdi Khorasanchi

Received: date / Accepted: date

1 **Abstract** This article explores the application of a wind farm layout optimization
2 framework using a particle swarm optimizer to three benchmark test cases. The de-
3 veloped framework introduces an increased level of detail characterizing the impact
4 that the wind farm layout can have on the levelized cost of energy by modelling the
5 wind farm's electrical infrastructure, annual energy production, and cost as functions
6 of the wind farm layout. Using this framework, this paper explores the application of
7 a particle swarm optimizer to the wind farm layout optimization problem considering
8 three different levels of wind farm constraint faced by modern wind farm developers.

Ajit C. Pillai
Industrial Doctorate Centre for Offshore Renewable Energy (IDCORE),
The University of Edinburgh, Edinburgh, UK
Present address: of Ajit C. Pillai
Renewable Energy Group,
University of Exeter, Penryn, UK
E-mail: a.pillai@exeter.ac.uk

John Chick
Institute for Energy Systems,
The University of Edinburgh, Edinburgh, UK
E-mail: john.chick@ed.ac.uk

Lars Johanning
Renewable Energy Group,
University of Exeter, Penryn, UK
E-mail: l.johanning@exeter.ac.uk

Mahdi Khorasanchi
Department of Mechanical Engineering,
Sharif University of Technology, Tehran, Iran
E-mail: khorasanchi@sharif.edu

9 The particle swarm optimizer is found to yield improvements in the layout with respect
10 to the levelized cost of energy for the three benchmark cases when compared to two
11 past studies. This highlights both applicability of the particle swarm optimizer to the
12 problem and the ways in which a wind farm developer could make use of the present
13 framework in the development and design of future wind farms.

14 **Keywords** offshore wind · layout optimization · particle swarm optimization · wind
15 farm design

16 1 Introduction

17 As the world transitions to a more sustainable energy sector, wind energy and in
18 particular offshore wind farms represent a significant means for reducing the greenhouse
19 gas emissions of electricity generation. As the offshore wind energy industry has grown,
20 both the size of wind farms and the size of individual turbines have grown significantly.
21 Wind farms now represent much larger projects both in terms of the area they cover
22 and their generational capacity than the early projects of last decade. With many
23 projects currently in development, it has become increasingly important to ensure that
24 these wind farms are designed in a sophisticated manner making use of the available
25 area as efficiently as possible.

26 To meet this need, tools have been developed exploring the optimal placement of
27 wind turbines, offshore substations, and intra-array cables within an offshore wind farm.
28 The original work in wind farm layout optimization done by Mosetti et al (1994) laid
29 the ground work for this field introducing a general approach that following work has
30 continued to utilize. This approach includes the assessment of both the energy produced
31 by a wind farm and the cost of the wind farm over the lifetime of the project. More
32 recent work in the field of offshore wind farm layout optimization has explored the
33 applicability of different optimization algorithms as well as the inclusion of additional
34 constraints and more detailed cost functions that a developer may face. The most
35 frequent optimization algorithm applied to the wind farm layout optimization problem
36 has been the genetic algorithm with several studies exploring its applicability to the

37 problem as posed by Mosetti et al (1994) and to more complex extensions (Chen et al,
38 2013; Couto et al, 2013; Elkinton, 2007; Elkinton et al, 2008; Geem and Hong, 2013;
39 Grady et al, 2005; Huang, 2009; Mittal, 2010; Shakoor et al, 2016; Zhang et al, 2014). In
40 a similar vein, recent studies have also explored optimization algorithms such as viral
41 based optimization (Ituarte-Villarreal and Espiritu, 2011), pattern search (DuPont
42 and Cagan, 2012), mixed-integer linear programming (Fagerfjäll, 2010), Monte Carlo
43 method (Marmidis et al, 2008), and random search (Feng and Shen, 2015) applied to
44 the wind farm layout optimization problem.

45 An optimization algorithm that has emerged as relevant to this problem and has
46 frequently been deployed for variations on this problem is the particle swarm optimizer
47 (PSO) (Chowdhury et al, 2012, 2013; Hou et al, 2017; Pookpant and Ongsakul, 2013;
48 Wan et al, 2010a,b). These existing studies have included various considerations be-
49 yond the problem originally defined in the seminal work in the field by Mosetti et al
50 (1994) such as hub height variations, turbine capacity variations, and intra-array cable
51 routing (Chowdhury et al, 2013; Feng et al, 2016; Hou et al, 2017). However, these
52 have still not considered several elements that would be important to a real wind farm
53 developer.

54 The present work, therefore, builds on the standard paradigm in wind farm layout
55 optimization by considering not only the impact the wind farm layout has on the
56 energy produced by the wind farm, but also the impact of layout design and turbine
57 placement on the electrical infrastructure and the wind farm's lifetime costs. Extending
58 the previous work in this field as well as that of the authors (Pillai et al, 2016b), the
59 present work presents this optimization problem with the inclusion of three constraint
60 sets of interest to wind farm developers and applies these to a series of benchmark
61 cases in which the levelized cost of energy (LCOE), a single metric that considers the
62 wind farm energy output and costs over the wind farm's lifetime, is used to compare
63 layouts.

64 This paper introduces increased detail in the evaluation a wind farm layout as well
65 as additional constraint levels that a developer will face in the design of a real offshore

66 wind farm, thereby striving to capture the impacts the wind farm layout can have
67 on the LCOE and explores the optimization of wind farm layouts using a cooperative
68 population based metaheuristic optimization approach¹, particle swarm optimization.
69 This therefore involves returning to the key reference work by Mosetti et al (1994)
70 and Grady et al (2005) and demonstrating that with the increased level of detail in the
71 evaluation function and the three different constraint sets, a particle swarm optimizer is
72 not only a relevant optimization algorithm, but is capable of identifying improvements
73 to the layouts regardless of the size of wind farm.

74 Section 2 introduces the approach of the wind farm layout optimization framework
75 describing the components and the optimization algorithm deployed. Section 3 intro-
76 duces the specific cases explored in this paper with the results presented in Section 4.
77 Section 5 analyses these results before the conclusions of this study are summarized in
78 Section 6.

79 **2 Approach**

80 In general, wind farm layout optimization requires two principal components, one for
81 assessing the quality of a given wind farm layout and a second for altering the layouts
82 in an effort to improve them. The standard paradigm for the optimization of wind farm
83 layouts makes use of the LCOE for assessing the quality of the layout, integrating wind
84 farm wake models and cost models in order to ascertain the LCOE for a given layout.
85 In this application, lower LCOE values represent better layouts. The present method-
86 ology expands on the standard paradigm by including the electrical infrastructure as
87 the initial step in the determination of the LCOE. The location of the offshore substa-
88 tions and the design of the intra-array cable network impacts both the annual energy
89 production (AEP) and the costs and is therefore an important step in assessing the
90 impact of changes to the turbine layout. The modular design of the approach, shown in
91 fig. 1, has allowed different wake, cost, and optimization algorithms to be implemented

¹ A *metaheuristic optimization approach* is a general strategy that is applicable to a wide range of optimization problems by making few or no assumptions about the problem (Burke and Kendall, 2013).

92 as part of the development of the tool. Prior to integration through the optimization
 93 algorithm, each of the components of the evaluation function have been independently
 94 validated (Pillai et al, 2016a, 2014, 2015). The optimization algorithm, the PSO in the
 95 present work, then makes use of the LCOE values in order to advise the next iteration
 96 of proposed layouts.

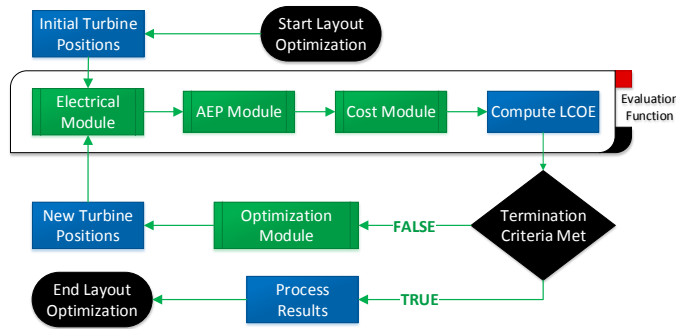


Fig. 1: Modular approach to wind farm layout optimization.

97 Existing offshore wind farms have generally been designed using simple spacing
 98 rules with turbines laid out along regular grids. Though this is the preferred approach
 99 from the perspective of search and rescue practitioners and helps to maintain naviga-
 100 tional routes through the wind farm, it does limit the designs that a developer could
 101 deploy (NOREL Group, 2014). In order to explore the different levels of constraints
 102 under which wind farms are currently being designed, allowing greater flexibility to the
 103 wind farm developer, three constraint sets are implemented each requiring a different
 104 optimization problem to be implemented. Under these constraints, the wind turbine
 105 positions are either on a fixed grid defined by the optimizer, one of a set of pre-defined
 106 allowable turbine positions, or anywhere within the wind farm area that satisfies the
 107 seabed constraints. These varying degrees of constraint on the wind farm design repre-
 108 sent the different approaches taken by European regulators in order to offer flexibility
 109 to the wind farm developers while still accounting for the interests and concerns of
 110 other marine stakeholders.

111 2.1 Evaluation of LCOE

112 As described, the wind farm layout optimization tool compares layouts on a basis of
 113 LCOE as this is a single metric which represents the cost effectiveness of a layout.
 114 The LCOE, measured in energy generation per unit cost, takes into account both the
 115 lifetime energy production of the wind farm and the lifetime costs of the project and
 116 is a common metric used by project developers to compare designs and competing
 117 projects. The energy production and costs are both discounted in order to represent
 118 the total lifetime energy production and lifetime costs in present value terms. In this
 119 way, the LCOE represents the ratio of the present value of the inputs to the present
 120 value of the outputs of the wind farm (Tegen et al, 2012, 2013).

$$LCOE = \frac{\sum_{t=1}^n \frac{C_t}{(1+r)^t}}{\sum_{t=1}^n \frac{AEP}{(1+r)^t}} \quad (1)$$

121 where C_t is the total costs incurred in year t , n is the project lifetime, AEP_t , is
 122 the annual energy production in year t , and r is the discount rate of the project.

123 2.1.1 Electrical Infrastructure Design

124 The first step in the evaluation of a layout as shown in fig. 1 is the design of the
 125 necessary electrical infrastructure to support the given layout considering any seabed
 126 restrictions which may be present at the site. As the electrical infrastructure impacts
 127 the energy produced by the wind farm due to losses through the electrical system, and
 128 changes to the electrical infrastructure can impact the project costs, the inclusion of
 129 this step helps quantify the impact on the LCOE of changes to the wind farm lay-
 130 out. The methodology for this is described in greater detail by the authors in Pillai
 131 et al (2015). The majority of existing wind farm layout optimization tools have not
 132 considered the impact of the turbine layout on either the intra-array cable collection
 133 networks or substation positions and the impact that these changes will have on the
 134 LCOE (Chen et al, 2013; Chowdhury et al, 2013; Couto et al, 2013; DuPont and Cagan,

135 2012; Elkinton, 2007; Elkinton et al, 2008; Geem and Hong, 2013; Grady et al, 2005;
136 Huang, 2009; Ituarte-Villarreal and Espiritu, 2011; Marmidis et al, 2008; Mosetti et al,
137 1994; Réthoré et al, 2011; Shakoor et al, 2016; Zhang, 2013; Zhang et al, 2014). The
138 existing tools that have included this step in the optimization of a wind farm layout,
139 have, however, omitted bathymetric constraints which a real-world developer would
140 face (Feng et al, 2016; Hou et al, 2017). Furthermore, existing standalone tools have
141 explored the optimization of the intra-array cable network for an offshore wind farm
142 as an independent problem. These approaches have similarly, also not considered the
143 irregular seabed exclusion areas for intra-array cables which arise from both bathymet-
144 ric and regulatory constraints that the developer may face at sites. As these exclusion
145 areas are often non-convex polygons in shape, their accurate inclusion in previous work
146 has proven challenging (Bauer and Lysgaard, 2015; Dutta and Overbye, 2013; Lindahl
147 et al, 2013; Rodrigues et al, 2016).

148 The optimization of the electrical infrastructure as developed in Pillai et al (2015)
149 uses of a series of heuristics and is therefore not guaranteed to identify the proven
150 optimal solution, however, it has been found to identify good quality solutions in an
151 acceptable runtime thereby representing a pragmatic approach to this real-world prob-
152 lem. This optimization process identifies not only the substation positions, and cable
153 paths given the bathymetric constraints, but also the conductor sizes for each electri-
154 cal cable in the network. This methodology to optimize the electrical infrastructure is
155 shown in algorithm 1.

156 The first step in this process is the determination of the substation positions by
157 clustering the turbine positions. By making use of a modified clustering algorithm
158 based on *k-means++* (Arthur and Vassilvitskii, 2007), the clustering process is capable
159 of generating substation positions which adhere to the seabed constraints and their own
160 capacity constraints while still minimizing the distance to the turbines. From here, a
161 pathfinding algorithm is executed to generate the fully connected set of cable paths for
162 the given turbine and substation positions. The pathfinding algorithm is used in order
163 to consider the seabed obstacles which define where the cables cannot be placed. Using

Algorithm 1 Offshore Wind Farm Intra-Array Cable Optimization

Require: The turbine positions, the GIS obstacles, and the number of substations

- 1: Given the number of substations assign each turbine to a substation and compute the substation positions using the *Capacitated kmeans++ Clustering*
 - 2: **for** all substations **do**
 - 3: **for** all turbines assigned to substation **do**
 - 4: Identify the 10 closest turbines
 - 5: Identify the constrained shortest path between the turbine and substation using *Delaunay Triangulation Based Navigational Mesh Pathfinding*.
 - 6: **for** 10 closest turbines **do**
 - 7: Identify the constrained shortest path between turbine pair using *Delaunay Triangulation Based Navigational Mesh Pathfinding*.
 - 8: **end for**
 - 9: **end for**
 - 10: Formulate mixed-integer linear program for substation and its assigned turbines given the 11 possible arcs for each turbine computed above
 - 11: **repeat**
 - 12: Solve *mixed-integer linear program*
 - 13: **if** any cables in mixed-integer linear program solution cross **then**
 - 14: Add individual crossing constraints
 - 15: **end if**
 - 16: **until** No cables cross
 - 17: **end for**
 - 18: **return** substation positions, cable paths, cable flows, and cable types
-

164 the accurate lengths of cables determined by the pathfinding algorithm, a capacitated
 165 minimum spanning tree (CMST) problem is formulated and solved using a commercial
 166 MILP solver, Gurobi (Gurobi Optimization Inc., 2015). The solution to the CMST
 167 identifies which of the cables should be deployed in the final network. In this way, the
 168 pathfinding step defines all the possible cables to consider and their accurate lengths,
 169 while the construction of the CMST selects which of these cables should be used to
 170 minimize the cost of the infrastructure. Following this, the pathfinding algorithm is
 171 again deployed to determine the export cable path from each substation now consider-
 172 ing the intra-array network as constraint regions to ensure that the export cable does
 173 not cross any of the intra-array cables.

174 Using this sub-tool, the electrical constraints of the cables and substations are not
 175 only taken into account, but seabed features dictating where this equipment cannot
 176 be placed are also considered. As intra-array cables can exceed £500,000 per kilometre
 177 installed, it is important that the impact the wind farm layout has on the amount

178 of cable needed is included in the assessment of the layout's cost (Gaillard, 2015).
179 Furthermore it is not uncommon for large offshore wind farms to be characterized
180 by a number of constraint regions which can significantly impact the design of the
181 intra-array collection network (Pillai et al, 2015).

182 *2.1.2 AEP Estimation*

183 It is well understood that any device extracting energy from a natural flux has some
184 impact on that flux. Wind turbines are no different, and directly behind an operating
185 wind turbine, the air flow is affected due to the extraction of energy. In this region,
186 known as the wake, the wind is characterized by reduced speeds and increased levels
187 of turbulence compared to the conditions upstream of the turbine (Barthelmie et al,
188 2006, 2009; Makridis and Chick, 2013; Renkema, 2007). The layout of a wind farm can
189 therefore have a major impact on the wind speeds that each individual wind turbine
190 within the wind farm experiences and thereby the energy production of the farm as a
191 whole. As a result of this, it is important for the wind turbine wakes to be accounted for
192 both when estimating wind farm production figures and the LCOE of a given layout.

193 The calculation of the AEP within this tool is done using an industry standard
194 analytic approach in which the wake losses are accounted for using the Larsen wake
195 model (Larsen, 1988). This model has been selected as validation using site data demon-
196 strated that it represented a good compromise between computational intensity and
197 accuracy (Gaumond et al, 2012; Pillai et al, 2014). The Jensen wake model used in pre-
198 vious layout optimization work has been found in validation studies to under-estimate
199 the AEP and is therefore not as well suited for this work as the Larsen model (Gaumond
200 et al, 2012).

201 To compute the AEP, each wind speed and direction combination are stepped
202 through in turn. For each free wind speed and wind direction the analytic wake model
203 is used to update each turbine's experienced wind speed based on the performance
204 of all upwind turbines. From this, the wind turbine power curve is used to convert
205 the incident wind speed to the energy generated under the given conditions. For each

206 wind speed and direction combination, the energy losses through the electrical cable
 207 network are then computed based on each turbine’s individual contribution to the AEP
 208 and the total wind farm contribution to AEP under the given free-stream wind speed
 209 and direction is updated. This total production for each wind speed and direction
 210 combination is then scaled by the probability of occurrence of this combination for the
 211 site in question before being added to the AEP.

$$AEP = 8766 \times \sum_{d_i} \sum_{v_i} P(d_i, v_i) \times [E(d_i, v_i) - L(E(d_i, v_i))] \quad (2)$$

212 where d_i is the wind direction; v_i is the wind speed; $P(d_i, v_i)$ is the joint probability
 213 of d_i and v_i ; $E(d_i, v_i)$ is the energy production for the wind farm for the combination of
 214 incident wind speed and direction considering the wake losses; and $L(E(d_i, v_i))$ is the
 215 electrical losses associated with the wind speed and direction as a result of the intra-
 216 array cable network. These electrical losses are assessed using an IEC loss calculation
 217 based on IEC 60228 and IEC 60287 (IEC, 2006a,b). This methodology is similar to
 218 that used by commercial tools such as WindFarmer and WindPRO which include both
 219 the losses due to wakes and within the intra-array cable network (DNV GL - Energy,
 220 2014; Thøgersen, 2005).

221 2.1.3 Cost Assessment

222 The final step in the evaluation of the LCOE as shown in fig. 1 is the estimation of
 223 the costs over the lifetime of the project. Where previous tools have assumed a cost
 224 which scales with the number of turbines, the approach used in this tool seeks to more
 225 accurately capture the impact that the wind farm layout has on the lifetime costs.
 226 Layouts with the same number of turbines may therefore have different costs using
 227 this model as opposed to the cost model frequently deployed in layout optimization
 228 which represents the cost as a function of only the number of turbines.

229 The project costs are divided into eight principal cost centres with varying degrees
 230 of dependency to the wind farm layout as shown in table 1. The capital expenditure
 231 (CAPEX) elements are incurred either in the construction stage of the project or in

232 the case of decommissioning at the end of the project life and discounted appropriately
233 while the operational expenditure (OPEX) elements are incurred in each year of oper-
234 ation following the construction period and prior to the decommissioning period. The
235 decommissioning costs are categorized as decommissioning expenditure (DECEX) and
236 are incurred at the end of life during the decommissioning period during which there
237 is no OPEX incurred.

238 Each of these cost elements considers not only the turbine positions relative to
239 one another, but also the turbine positions relative to the construction and O&M
240 ports, as well as the depth at each individual turbine's position. Relevant cost centres
241 also consider the vessel parameters, cable parameters, and design parameters of the
242 substations. The specific cost relationships have been developed in discussions with
243 wind farm developers and suppliers in order to ensure that the costs are representative
244 of the costs to be incurred by future projects in European waters and accurately capture
245 the impact that the turbine layout can have on these costs.

246 *Turbine Supply* The cost associated with the supply of the turbines is based entirely on
247 a price per turbine supplied by turbine manufacturers. This cost is therefore independent
248 of the layout of the wind farm and factor only of the number of turbines or installed
249 capacity of the wind farm.

250 *Turbine installation* Using market values for vessel costs and their capacities, the tur-
251 bine installation costs are modelled by assessing the total amount of time required
252 to install the turbines at their specific locations within the wind farm. This therefore
253 includes the calculation of the time required for each installation operation, the travel
254 time between turbines, and the travel time to and from the construction port. In order
255 to determine the optimal vessel installation route, the turbines are clustered based on
256 the capacity of the installation vessel, and for each cluster a shortest path is computed
257 between the port, each turbine in the cluster, and the port again. This approach there-
258 fore accurately computes the distance that the vessel must travel over the installation
259 process. From this, the total time is computed based on assumed weather availability

260 and the costs computed based on the vessel and equipment day rates. The turbine
261 layout, therefore, has a direct impact on the time needed to travel between turbine
262 positions as well as to and from the port.

263 *Foundation supply* Foundation costs are found to be highly dependent on the site
264 conditions where the foundation is to be installed. To account for this dependence,
265 previous cost models have attempted a bottom up approach based on the soil char-
266 acteristics at the installation site to model the costs. Unfortunately this approach has
267 proven difficult to validate for all foundation types (Elkinton, 2007). For the present
268 tool therefore, a depth dependency has been developed from discussions with manufac-
269 turers and the specific soil conditions are not included. Detailed bathymetry of a site is
270 therefore necessary in order to accurately estimate the variation in foundation supply
271 costs as a function of the turbine layout. As the original cases defined by Mosetti et al
272 (1994) did not include bathymetric data, a constant depth has been assumed across
273 the site.

274 *Foundation installation* The foundation installation process like the turbine installa-
275 tion module is based on estimating the time needed to complete the operations and
276 converting this time to a cost. Unlike the turbine installation though, this is modelled
277 as three distinct phases which each uses a different vessel to complete.

278 Regardless of the foundation type (gravity-based, monopile, or jacket), some seabed
279 preparation is necessary. For a gravity-based foundation this might be the necessary
280 dredging and levelling of the seabed, while for monopiles and jackets this would more
281 likely be pre-pilling works including surveying and drilling. After this step, the foun-
282 dations will be installed as a separate operation following which some kind of scour
283 protection will often be added. The installation of scour protection is again modelled as
284 a separate step involving a different vessel from either the site preparation or foundation
285 installation processes. In some conditions, the scour protection will not be necessary,
286 however, for the time being the present model assumes that all turbines will require
287 scour protection.

288 *Intra-array cable costs* The total horizontal length of intra-array cables required is
289 computed from the intra-array cable optimization tool described earlier. This tool is
290 described in detail in previous work by the authors (Pillai et al. 2015). This tool has the
291 support for optimizing the layout for different cable cross-section sizes and therefore can
292 output not only the total length of cable, but the horizontal lengths required for each
293 segment and the required cross-section. From this, the intra-array cable cost module
294 computes the necessary vertical cable and the necessary spare cable before computing
295 the costs.

296 Following the calculation of the supply cost, the installation cost is computed in a
297 similar manner to the turbine and foundation installation modules. This is done based
298 on data available for cable trenching vessels and therefore assumes that all cables are
299 trenched and buried.

300 *Operations and Maintenance* The operations and maintenance costs are based on a
301 tool developed by EDF Energy R&D UK Centre which models the anticipated oper-
302 ations and maintenance cost of a project to vary with the projects distance from the
303 operations and maintenance port and the capacity of the project. As this term is af-
304 fected by distance of the wind farm to the operations and maintenance port, this too is
305 affected by the layout. The operations and maintenance costs are classed as operational
306 expenditure (OPEX) as these are incurred each year of operation as opposed to the
307 preceding cost elements which are only incurred during the construction period and
308 are therefore classed as CAPEX elements.

309 *Decommissioning* The decommissioning costs include the removal of the turbines and
310 foundations. At the moment, it is unclear what will happen to the transmission and
311 export cables at the end of a wind farm's life. The model therefore assumes that
312 these cables are not removed at the time of decommissioning, but simply cut at the
313 turbines and substation, leaving the buried lengths as they are. The decommissioning
314 costs are therefore modelled similar to the installation processes with the time each
315 vessel is required first computed before this is converted to a cost. Like the installation

316 processes it is assumed that the vessels have some finite capacity and must return to
 317 the decommissioning port during the overall operation. The turbines and foundations
 318 are assumed to be decommissioned in separate steps requiring separate vessels. Like
 319 the installation phases, this term is therefore dependent on the turbine positions and
 320 is affected by the proposed layout.

321 *Offshore Transmission Assets* The final cost element of this cost model is the inclu-
 322 sion of the offshore transmission asset transfer fees. In the UK, the offshore substation,
 323 export cables, and onshore substation must be owned and operated by a separate com-
 324 pany from the wind farm operator. Practically, therefore, most wind farm developers
 325 build these assets, and then transfer them to a transmission operator before commis-
 326 sioning the wind farm. As a result, only some of the CAPEX is incurred by the project,
 327 and the rest is incurred as a component of the transmission fee along with regionally
 328 based costs set by the network operator, in the UK this is National Grid. Both the
 329 CAPEX and OPEX components of the Offshore Transmission Owners assets have been
 330 computed in discussion with National Grid and equipment manufacturers based on the
 331 capacity of the assets.

Table 1: Cost Contribution to CAPEX and OPEX

Cost Element	CAPEX	OPEX	DECEX	Inclusion of Layout
Turbine Supply	✓	-	-	Low
Turbine Installation	✓	-	-	Medium
Foundation Supply	✓	-	-	Medium
Foundation Installation	✓	-	-	Medium
Intra-Array Cables	✓	-	-	High
Operations and Maintenance (O&M)	-	✓	-	Medium
Decommissioning	-	-	✓	Medium
Offshore Transmission Assets	✓	✓	-	Low

332 2.2 Particle Swarm Optimization

333 The particle swarm optimization algorithm is a population based metaheuristic based
 334 on the behaviour of flocking birds or shoaling fish (Eberhart and Kennedy, 1995;
 335 Kennedy and Eberhart, 1995). In this respect, the algorithm treats the candidate so-
 336 lutions as particles within a swarm which are exploring the search space cooperatively.
 337 Each particle (solution) changes its position in the search space between iterations
 338 based on a velocity vector defined by the knowledge of both the swarm's past position
 339 and the individual particle's historical positions within the search space. For iteration
 340 i of the process, this velocity, v , for a given particle is given by:

$$v_i = C_1 \times v_{i-1} + C_2 \times r_1 (p - x_i) + C_3 \times r_2 (g - x_i) \quad (3)$$

341 where C_1 , C_2 , and C_3 are coefficients representing the weighting of each of the
 342 contributors determined by tuning the PSO; p is the best position that the particle has
 343 historically occupied within the search space; g is the best position that any individual
 344 within the swarm as a whole has ever occupied; x is the solution under consideration;
 345 and r_1 and r_2 are two random numbers between 0 and 1 selected using a uniform
 346 distribution. With this velocity the particle's position the next iteration is given by:

$$x_{i+1} = x_i + v_i \quad (4)$$

347 Once each particle's position is updated, the evaluation function is used to de-
 348 termine the corresponding LCOE for each of the proposed layouts. Each particle's
 349 historical best position p is then updated if needed, and the best p value is used to
 350 define g . These updated p and g values are needed in the determination of the updated
 351 particle velocities for the next iteration of the process.

352 Compared to the genetic algorithm or alternate metaheuristics which have been
 353 applied to the wind farm layout optimization problem, the PSO is of interest as in op-
 354 timization benchmarking studies it has been found to find high quality solutions in less
 355 time than a similar genetic algorithm (Eberhart et al, 2001; Hassan et al, 2005). Given

the complexity of future wind farms, this is of interest to wind farm developers as the PSO could therefore identify better solutions than the industry standard approaches using commercial software tools thereby leading to more efficient wind farm layouts. Furthermore, where the genetic algorithm is seen as a competitive metaheuristic in which individual solutions compete for survival, the PSO fosters a cooperative environment where the individual solutions directly impact one another. In this way, all members of the swarm are made aware of the improvements found by each individual particle, using this information to inform their future movements within the search space.

The parameters of the present PSO are given in table 2. Due to the available computational power, this study used a constant swarm size of 100 particles. In order to ensure that the velocity vector does not take a particle outside of the search space, a dynamic velocity clamping approach was used in which velocity limits are imposed in each direction based on the location of the particle. This is similar to the trajectory constriction approach described by Clerc and Kennedy (2002); Van Den Bergh and Engelbrecht (2006). For the binary constraints described below, a binary implementation of the PSO in which all decision variables are binary variables is necessary. As the velocity in the binary implementation must correspond to a specific decision variable being either a 1 or a 0, a velocity transfer function is required to convert the velocity for each decision variable into a probability that the decision variable should be a 1.

Table 2: Particle Swarm Parameters

Parameter	Description
Swarm Size	100
Velocity Clamping	Dynamic
Velocity Transfer Function (Binary Encoding)	$T(x) = \left \frac{2}{\pi} \times \arctan \left(x \cdot \frac{\pi}{2} \right) \right $
Neighbourhood Topology	Global (gBest)
Stop Criteria	Diversity <10%
	Maximum generations reached
	No improvement over 50 generations

376 In the original study by Mosetti et al (1994), the wind farm area was discretized
377 into 100 allowable turbine positions. The optimizer is therefore tasked with the selec-
378 tion of which of these positions to use for the deployed wind turbines. This therefore
379 represents a constraint on the turbine placement and it would be expected that better
380 layouts could be achieved if this constraint was relaxed. To explore this, three different
381 constraints on the turbine placement are used in the present study:

- 382 1. **Array constraints** - The turbine positions are constrained to being on a regular
383 grid with constant downwind and crosswind spacings. The decision variables of
384 the optimization problem define the spacing and orientation of the regular grid of
385 turbine positions with constant downwind and crosswind spacing throughout the
386 site.
- 387 2. **Binary constraints** - The turbine positions are limited to being one of a predefined
388 set of allowable turbine positions. For the present study, the wind farm area is
389 discretized into 100 allowable turbine positions as defined Mosetti et al (1994) and
390 the decision variables of the optimization problem are binary variables representing
391 the presence of a turbine in a particular cell. This represents the case in which the
392 wind farm developer, regulator, and stakeholders define a set of acceptable turbine
393 positions and the wind farm is designed by selecting turbine positions from this
394 set.
- 395 3. **Continuous constraints** - The turbine positions can be anywhere within the wind
396 farm boundary that is technically feasible. The decision variables directly define the
397 turbine coordinates and may therefore occupy any value within the wind farm area.
398 This represents a situation in which the wind farm developer is free to design the
399 wind farm as they see best limited only by the technical constraints of the site.

400 The three approaches represent different ways in which the problem can be defined
401 all of which are used by wind farm developers to design and explore the available
402 options in the design of an offshore wind farm. The array and binary constraint sets are
403 of interest to a wind farm developer in regions where the regulator imposes some degree
404 of symmetry as a result of navigational and search and rescue safety concerns (NOREL

405 Group, 2014). As the three constraint sets have fundamentally different degrees of
406 complexity and represent different design spaces the optimizers were tuned individually
407 for each of the problems in an attempt to maximize the performance though the same
408 swarm size was used for all cases. Regardless of the placement constraints used, the
409 technical seabed constraints such as the position of wrecks, unexploded ordnance, and
410 the seabed slope are considered. For all three constraint sets, a minimum separation
411 constraint is applied to ensure that turbines do not risk colliding and the wind farm
412 boundary explicitly defines the limits of the wind farm.

413 3 Definition of Cases

414 In the development of layout optimization tools three case studies have been defined by
415 Mosetti et al (1994). These three cases have been commonly used in order to evaluate
416 the performance and demonstrate the capabilities of wind farm layout optimization
417 tools. In order to demonstrate the capabilities of the present framework, which makes
418 use of a more detailed layout evaluation function, the three cases are approached us-
419 ing the original constraints as well as under two different sets of relaxed constraints.
420 Through this, the capabilities of the present framework using a PSO are highlighted.

421 The three cases all consider a 2 km by 2 km area in which turbines must be placed,
422 however, they differ with regards to the wind resource. Case one considers a case
423 of *constant wind speed and constant wind direction* in which the wind is constantly
424 12 m s^{-1} and from the 10° sector centred on 0° . The second case is described as the
425 case of *constant wind speed and variable direction* in which the wind is again constantly
426 12 m s^{-1} , but now has an equal probability of blowing from any of the 36 discrete
427 wind directions. Finally, the third case, the case of *variable wind speed and direction*,
428 describes a case in which both the wind speed and wind direction are variable and
429 most closely resembles a true wind farm. All three cases describe the resource using
430 36 discrete wind directions which are each used in the calculation of the AEP and
431 the modelling of the wakes in the evaluation function. Validation studies of analytic
432 wake models have found that these models are not necessarily more accurate when

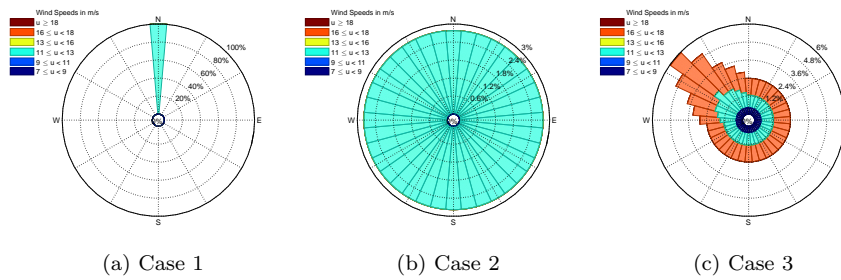


Fig. 2: Wind roses for the three different resource cases.

433 using narrower wind direction sectors, and discrete wind sectors of 10° to 30° in size
 434 should be used when deploying analytic wake models such as the Jensen or Larsen
 435 models (Gaumond et al, 2013; Pillai et al, 2014).

436 The original cases do not define the water depth nor are the locations of the relevant
 437 ports defined. In order to allow comparison with existing results for these case studies,
 438 the water depth has been assumed constant across the site and the ports have been
 439 placed far away relative to the size of the wind farm.

440 4 Results

441 In order to demonstrate the capabilities of the present framework using a PSO, the
 442 final layouts from the original study by Mosetti et al (1994) and the final layouts from
 443 a subsequent study by Grady et al (2005) are evaluated using the present evaluation
 444 function in order to offer a fair comparison to the new layouts proposed. These two
 445 studies used different numbers of turbines for each resource case and therefore cannot
 446 be directly compared to one another. Likewise, much of the literature has also allowed
 447 the number of turbines to vary thereby making direct comparisons challenging. In the
 448 present framework, the number of turbines is fixed thereby allowing a direct comparison
 449 on the same number of turbines against both the reference case study and the different
 450 constraint sets.

451 The original layouts produced in the studies by Mosetti et al (1994) and Grady
 452 et al (2005) for all three resource cases are shown in fig. 3. The studies performed by

453 Mosetti et al (1994) and Grady et al (2005) both allowed the number of turbines to
 454 vary and therefore for each of the resource cases, the two studies present different wind
 455 farm sizes. In the present study, each wind farm resource is executed with all three sets
 456 of constraints and at same the wind farm sizes as reported in the two past studies in
 457 order to fairly compare to the reference studies. The binary constraint set, represents
 458 the most similar case to the problem originally defined by Mosetti et al (1994), however,
 459 the present tool uses a fixed number of turbines, while the original studies allowed this
 460 to change. Each of the presented optimization results represents the converged results
 461 after a maximum of 100 generations. In general, less than 60 generations were required
 462 to reach the converged results presented.

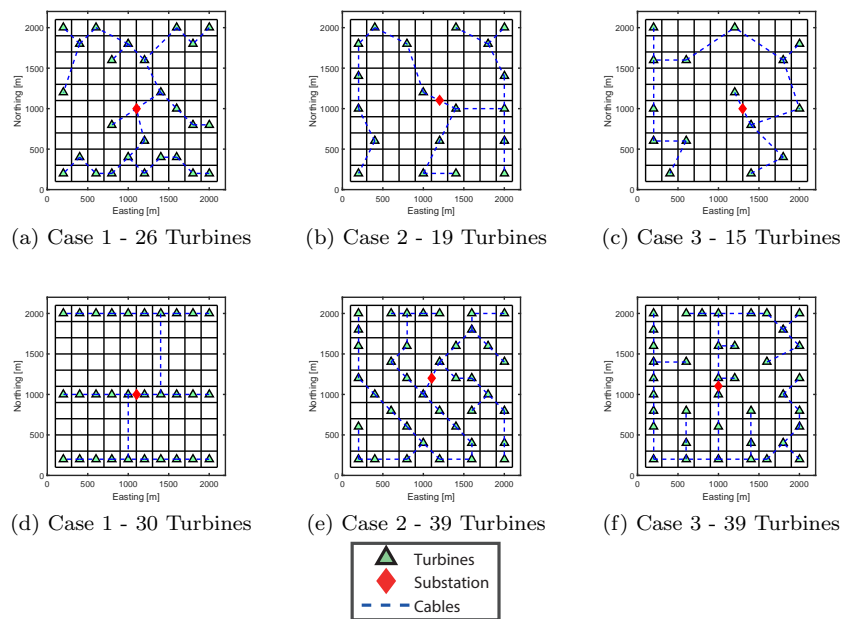


Fig. 3: Original optimized layouts proposed by Mosetti et al (1994) on the top row and Grady et al (2005) on the bottom row for the three resource cases.

463 4.1 Case 1: Constant Wind Speed, Constant Direction

464 The results presented in table 3 shows the outputs from re-evaluating the original
465 layouts proposed in the previous studies (Grady et al, 2005; Mosetti et al, 1994) as
466 well as the outputs from the execution of the PSO for this case. As the developed
467 method uses the number of turbines as an input to the optimization process, it was
468 necessary to execute the optimizer for two different wind farm sizes corresponding
469 to the studies originally performed by Mosetti et al (1994) and Grady et al (2005)
470 respectively, allowing the results to be directly compared to these past studies (shown
471 in figs. 3a and 3d). As described above, each of the wind farm sizes was run with three
472 different types of constraints corresponding to different requirements on the placement
473 of the turbines.

Table 3: Layout Optimization Results: Constant Wind Speed, Constant Direction

Study	Number of Turbines	Lifetime Cost [£]	AEP [MWh]	LCOE [£/MWh]
Mosetti et al (1994)	26	4.42×10^8	9.90×10^4	522.87
Array Constraints	26	4.39×10^8	1.18×10^5	434.87
Binary Constraints	26	4.41×10^8	1.01×10^5	510.46
Continuous Constraints	26	4.42×10^8	1.16×10^5	447.18
Grady et al (2005)	30	4.77×10^8	1.13×10^5	496.29
Array Constraints	30	4.76×10^8	1.33×10^5	419.61
Binary Constraints	30	4.77×10^8	1.13×10^5	496.29
Continuous Constraints	30	4.78×10^8	1.33×10^5	421.64

474 From the results presented in table 3 it can be observed that for both wind farm
475 sizes, the PSO either finds improvements or the same solution proposed by the refer-
476 ences cases regardless of which constraint set was used. Specifically, using the binary
477 constraint set for the larger wind farm size resulted in the same layout presented by
478 Grady et al (2005) whereas for each of the other five cases, improvements were high-
479 lighted compared to the relevant reference case. As is highlighted in table 3, for both
480 wind farm sizes, the variation in costs as a result of the changes in layout are very small
481 as the micrositing within the 4 km^2 wind farm area results in very minimal changes

482 in the installation costs. In fact, as the port position was not defined in the original
 483 case, it was necessary to place the port very far away relative to the size of the wind
 484 farm in order to remove any bias to the port's position. As a result of this, there are
 485 relatively large transit times to the wind farm included in each installation cost which
 486 are unaffected by the wind farm layout, but a function of the wind farm's distance
 487 from the installation port.

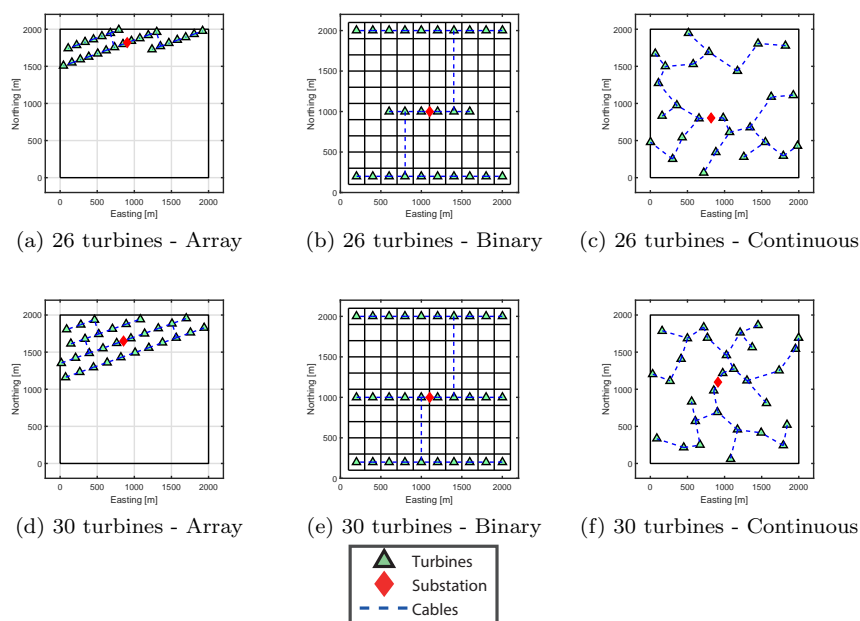


Fig. 4: Optimized layouts for the case of a constant wind speed and constant direction with 26 turbines (top row) and 30 turbines (bottom row) using both optimization algorithms and all three constraint sets.

488 4.2 Case 2: Constant Wind Speed, Variable Direction

489 The results for each of the constraint sets and wind farm sizes are summarized in table 4
 490 and the corresponding layouts are shown in fig. 5. The original layouts proposed by
 491 the reference studies are shown in figs. 3b and 3e. From table 4, it can be seen that

492 similar to the results for Case 1, the newly developed layout optimization framework
 493 for offshore wind farms is capable of identifying improvements using the PSO under
 494 all three constraint sets for both wind farm sizes.

Table 4: Layout Optimization Results: Constant Wind Speed, Variable Direction

Study	Number of Turbines	Lifetime Cost [£]	AEP [MWh]	LCOE [£/MWh]
Mosetti et al (1994)	19	3.77×10^8	8.17×10^4	540.25
Array Constraints	19	3.77×10^8	8.32×10^4	530.79
Binary Constraints	19	3.77×10^8	8.21×10^4	537.49
Continuous Constraints	19	3.77×10^8	8.19×10^4	538.29
Grady et al (2005)	39	5.62×10^8	1.57×10^5	419.13
Array Constraints	39	5.61×10^8	1.61×10^5	408.07
Binary Constraints	39	5.61×10^8	1.59×10^5	413.00
Continuous Constraints	39	5.62×10^8	1.58×10^5	417.29

495 4.3 Case 3: Variable Wind Speed, Variable Direction

496 The results of executing the current framework with the PSO are found in table 5
 497 with the corresponding layouts plotted in fig. 6 and the original reference layouts in
 498 figs. 3c and 3f. Similar to the previous cases, the PSO using any of the constraint sets
 499 was capable of identifying improved layouts with regards to the LCOE. Similar to the
 500 previous cases, the best results were found using the array constraints.

501 5 Discussion

502 Using the present tool, cost variations as a result of changes to the wind farm layout
 503 are captured and included in the calculation of the layout's LCOE. For a small wind
 504 farm such as those considered here, it is, however, the increase in AEP which drives
 505 the decreases in LCOE, which is why for many cases an increase in lifetime cost is
 506 observed, however, the corresponding increase in AEP is sufficiently large to still result
 507 in a net reduction of the LCOE.

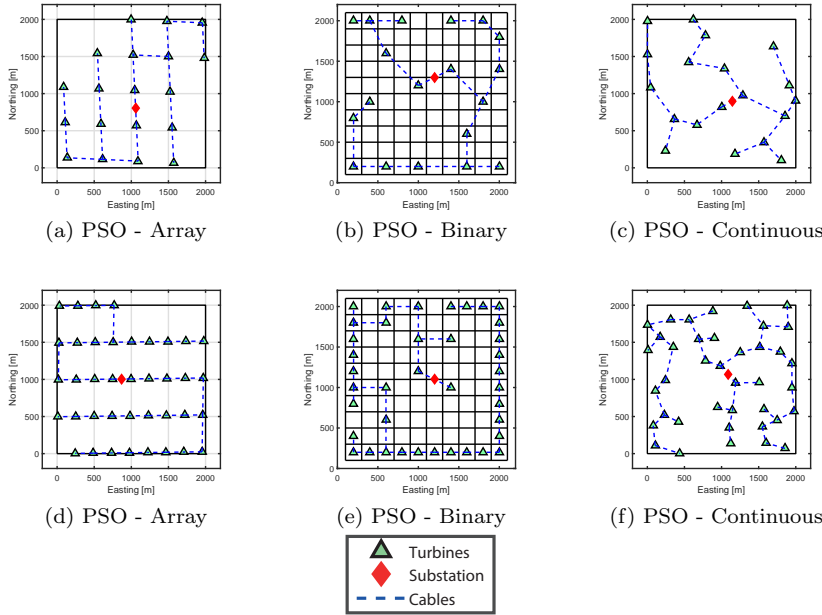


Fig. 5: Optimized layout for the case of a constant wind speed and variable direction with 19 and 39 turbines using both optimization algorithms and all three constraint sets.

Table 5: Layout Optimization Results: Variable Wind Speed, Variable Direction

Study	Number of Turbines	Lifetime Cost [£]	AEP [MWh]	LCOE [£/MWh]
Mosetti et al (1994)	15	3.40×10^8	6.89×10^4	576.94
Array Constraints	15	3.39×10^8	6.93×10^4	571.51
Binary Constraints	15	3.39×10^8	6.91×10^4	573.87
Continuous Constraints	15	3.39×10^8	6.91×10^4	574.22
Grady et al (2005)	39	5.62×10^8	1.74×10^5	377.14
Array Constraints	39	5.63×10^8	1.75×10^5	375.50
Binary Constraints	39	5.62×10^8	1.75×10^5	376.72
Continuous Constraints	39	5.62×10^8	1.75×10^5	376.72

508 As would be expected, relaxing the turbine positioning constraints by designing
 509 arrays within the boundary or by treating the wind farm area as a continuous do-
 510 main, results in significant improvements in the LCOE as the shape of the layout can
 511 be designed to best utilize the characteristics of the site. Somewhat surprisingly, the

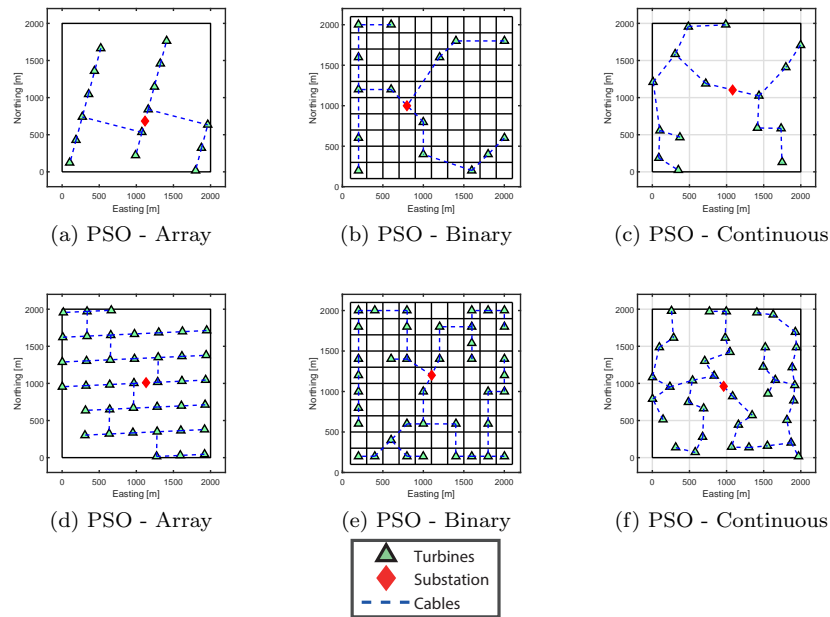


Fig. 6: Optimized layout for the case of a variable wind speed and variable direction with 15 and 39 turbines using both optimization algorithms and all three constraint sets.

512 continuous optimizer which represents the most unconstrained case was unable to con-
 513 sistently find improvements over the array optimizer. However, both were consistently
 514 able to find improvements compared to the binary optimizer which made use of the
 515 discretized wind farm area. Interestingly, the array optimizer appears more capable
 516 than the others to adjust the shape of the wind farm layout to take advantage of the
 517 wind resource.

518 As the array optimizer and continuous optimizer did not identify similar solutions
 519 it suggests that further tuning of the PSO is necessary in order to ensure that the
 520 optimizers are not prematurely converging to a local solution. Furthermore, given the
 521 results it indicates that moving from the binary or array optimizers to the continuous
 522 optimizer increases the size of the problem quite significantly. In the present case,
 523 all three constraint sets were solved using the same size of swarm, however, it might
 524 be more prudent for the swarm size to change depending on which constraint set is

525 used thereby allowing the more complex problem to be solved with a larger swarm
526 in order to avoid premature convergence. With a sufficiently large swarm, it should
527 be possible for the PSO to converge to a higher quality solution closer to that of
528 the global optimum. It should be noted, however, that metaheuristic algorithms like
529 the PSO cannot guarantee, especially for a complex objective function such as the
530 LCOE, that the optimization process will converge to the global optimum. Given the
531 computational power allocated for this study, however, it was not possible to execute
532 the optimizers with larger swarms. With swarms of 100 individuals as used in this
533 study, each optimization took between one and three days to execute depending on the
534 wind farm size and the selected constraints when executed on a desktop computer with
535 an Intel Xeon 8-CPU processor rated at 3.3 GHz. As the three different constraint sets
536 lead to three different instances of the problem with different decision variables, the
537 design spaces are not directly comparable and each of the three optimizers should be
538 tuned independently in order to ensure the best performance.

539 Looking at Case 1, it can be seen that both the binary and continuous optimizers use
540 the majority of the available space, while the array optimizer is capable of identifying
541 that it should sacrifice a close spacing in the direction perpendicular to the single
542 wind direction. The binary optimizer is unable to find a similar solution due to the
543 resolution of the discrete grid used in the binary optimization. This suggests that the
544 discretization of the wind farm area should be done at a higher resolution to afford
545 the optimizer a greater degree of flexibility. The present study used the 100 allowable
546 turbine positions as this is what had been used in past studies. Increasing the number
547 of allowable turbine positions through a higher resolution would, however, increase
548 the size of the problem and potentially slow the rate of convergence. The continuous
549 optimizer should, however, be capable of identifying a similar solution, and the fact
550 that it does not highlights that further work remains to be done with this optimizer in
551 order to ensure that high quality solutions are reached.

552 The results from Case 2, however, indicate that the binary optimizer is placing more
553 turbines on the edge of the wind farm in order to take advantage of the symmetrical

554 wind resource, especially in the larger wind farm case. For this resource case and the
555 larger wind farm, compared to the full continuous optimizer the binary optimizer results
556 in better AEP values, demonstrating that additional constraints on the problem can
557 reduce the search space without sacrificing the quality of the ultimate layouts.

558 Limiting the turbine positions to 100 possible positions significantly constrained
559 the search space such that the solutions had inferior fitness values compared to the
560 more relaxed constraint sets. This indicates that moving to the binary constraints with
561 a discretized set of turbine positions over-constrains the problem, eliminating high
562 quality valid solutions. Considering the Mosetti cases, the impact of this on the LCOE
563 varied from £1 per MWh to £70 per MWh increases, corresponding to 0-16% potential
564 improvements in LCOE from relaxing the constraints. Given some of the assumptions,
565 the percentage difference is smaller than it would be if this were a real site, as there
566 are some fixed costs which are intentionally overestimated. As described earlier, the
567 port location was defined as far away relative to the size of the wind farm in order to
568 avoid the optimizer clustering turbines close to the installation port. The installation
569 costs are therefore larger than they would be for a real case thereby increasing the
570 LCOE. For these cases, it is therefore more valuable to analyse the absolute difference
571 in LCOE rather than the percentage reduction.

572 Interestingly, Case 3 which represents the most realistic wind resource case finds
573 very small variations in AEP across the three different constraint sets demonstrating
574 that for a more varied wind speed and wind direction combinations all three constraint
575 sets have merit and are capable of finding good solutions. The choice of which constraint
576 set to use therefore becomes a function of what constraints are imposed on the site
577 developer by consenting agencies or other stakeholders. The results from this case
578 also demonstrate that there are several different layouts with similar AEP, cost and
579 LCOE values showing the complexity of the search space. Given that there are different
580 layouts which can result in similar solutions the tuning of the optimizer becomes more
581 important and further work will need to further explore this in order to ensure that the

582 optimization process is not overlooking significant improvements and that the optimizer
583 is operating in appropriate time scales.

584 **6 Conclusion**

585 This paper has presented the first results of an extended wind farm layout optimiza-
586 tion framework making use of a more detailed LCOE evaluation function than existing
587 layout optimization tools. This framework which makes use of a previously validated
588 LCOE evaluation function has been applied to three different case studies using three
589 different sets of placement constraints and two different wind farm sizes for each re-
590 source case in order to highlight both the applicability of a PSO given the increased
591 detail and the improvements that can be made relative to the reference studies. The
592 PSO applied to these three benchmark case studies have presented layouts with im-
593 proved LCOE compared to past studies using a genetic algorithm. Furthermore, the
594 results shown here indicate that the PSO is of interest to this area of research as the
595 results can be obtained at a lower computational cost compared to a genetic algorithm.

596 By using multiple constraint sets it is also shown that by limiting the optimizer to
597 create gridded layouts does not result in poor solutions, though the observed trends
598 highlight the need for further tuning of the PSO in order to insure that the optimizer
599 does not prematurely converge. Further work should explore both using multiple runs
600 rather than single runs in order to avoid any seeding bias as well as using additional
601 computational power thereby allowing larger swarms to be tested.

602 **Acknowledgements** This work is funded in part by the Energy Technologies Institute (ETI)
603 and RCUK energy program for IDCORE (EP/J500847/1) and supported by EDF Energy R&D
604 UK Centre.

605 **References**

606 Arthur D, Vassilvitskii S (2007) k-means++: The Advantages of Careful Seeding. Pro-
607 ceedings of the 18th Annual ACM-SIAM symposium on Discrete Algorithms New

-
- 608 Orleans, USA 8:1–11
- 609 Barthelmie RJ, Folkerts L, Larsen GC, Frandsen ST, Rados K, Pryor SC, Lange B,
610 Schepers G (2006) Comparison of Wake Model Simulations with Offshore Wind Tur-
611 bine Wake Profiles Measured by Sodar. *Journal of Atmospheric and Oceanic Technol-*
612 *ogy* 23(7):888–901, DOI 10.1175/JTECH1886.1, URL [http://journals.ametsoc.](http://journals.ametsoc.org/doi/abs/10.1175/JTECH1886.1)
613 [org/doi/abs/10.1175/JTECH1886.1](http://journals.ametsoc.org/doi/abs/10.1175/JTECH1886.1)
- 614 Barthelmie RJ, Hansen K, Frandsen ST, Rathmann O, Schepers JG, Schlez W, Phillips
615 J, Rados K, Zervos A, Politis ES, Chaviaropoulos PK (2009) Modelling and mea-
616 suring flow and wind turbine wakes in large wind farms offshore. *Wind Energy*
617 12(5):431–444, DOI 10.1002/we.348, URL <http://doi.wiley.com/10.1002/we.348>
- 618 Bauer J, Lysgaard J (2015) The Offshore Wind Farm Array Cable Layout Problem - A
619 Planar Open Vehicle Routing Problem. *Journal of the Operational Research Society*
620 66(3):1–16, URL <http://www.ii.uib.no/~joanna/papers/owfac1.pdf>
- 621 Burke EK, Kendall G (2013) *Search Methodologies*, 2nd edn. Springer US, Boston,
622 MA, DOI 10.1007/0-387-28356-0
- 623 Chen Y, Li H, Jin K, Song Q (2013) Wind farm layout optimization using genetic
624 algorithm with different hub height wind turbines. *Energy Conversion and Man-*
625 *agement* 70:56–65, DOI 10.1016/j.enconman.2013.02.007, URL [http://linkinghub.](http://linkinghub.elsevier.com/retrieve/pii/S0196890413000873)
626 [elsevier.com/retrieve/pii/S0196890413000873](http://linkinghub.elsevier.com/retrieve/pii/S0196890413000873)
- 627 Chowdhury S, Tong W, Messac A, Zhang J (2012) A mixed-discrete Particle Swarm
628 Optimization algorithm with explicit diversity-preservation. *Structural and Mul-*
629 *tidisciplinary Optimization* 47(3):367–388, DOI 10.1007/s00158-012-0851-z, URL
630 <http://link.springer.com/10.1007/s00158-012-0851-z>
- 631 Chowdhury S, Zhang J, Messac A, Castillo L (2013) Optimizing the arrange-
632 ment and the selection of turbines for wind farms subject to varying wind
633 conditions. *Renewable Energy* 52(315):273–282, DOI 10.1016/j.renene.2012.10.017,
634 URL <http://linkinghub.elsevier.com/retrieve/pii/S0960148112006544>
635 [http://www.sciencedirect.com/science/article/pii/S0960148112006544](http://linkinghub.elsevier.com/retrieve/pii/S0960148112006544)

-
- 636 Clerc M, Kennedy J (2002) The particle swarm - explosion, stability, and convergence in
637 a multidimensional complex space. *IEEE Transactions on Evolutionary Computation*
638 6(1):58–73, DOI 10.1109/4235.985692
- 639 Couto TG, Farias B, Diniz ACGC, Morais MVGD (2013) Optimization of Wind Farm
640 Layout Using Genetic Algorithm. 10th World Congress on Structural and Multidis-
641 ciplinary Optimization Orlando, USA pp 1–10
- 642 DNV GL - Energy (2014) WindFarmer Theory Manual. GL Garrad Hassan, URL
643 <https://www.dnvg1.com/services/windfarmer-3766>
- 644 DuPont BL, Cagan J (2012) An Extended Pattern Search Approach to Wind
645 Farm Layout Optimization. *Journal of Mechanical Design* 134(8):081,002, DOI 10.
646 1115/1.4006997, URL [http://mechanicaldesign.asmedigitalcollection.asme.
647 org/article.aspx?articleid=1484782](http://mechanicaldesign.asmedigitalcollection.asme.org/article.aspx?articleid=1484782)
- 648 Dutta S, Overbye T (2013) A graph-theoretic approach for addressing trenching
649 constraints in wind farm collector system design. 2013 IEEE Power and Energy
650 Conference at Illinois (PECI) Urbana-Champaign, USA pp 48–52, DOI 10.1109/
651 Peci.2013.6506033, URL [http://ieeexplore.ieee.org/lpdocs/epic03/wrapper.
652 htm?arnumber=6506033](http://ieeexplore.ieee.org/lpdocs/epic03/wrapper.htm?arnumber=6506033)
- 653 Eberhart R, Kennedy J (1995) A new optimizer using particle swarm theory. MHS'95
654 Proceedings of the Sixth International Symposium on Micro Machine and Human
655 Science pp 39–43, DOI 10.1109/MHS.1995.494215
- 656 Eberhart RCR, Yuhui Shi, Shi Y (2001) Particle swarm optimization: developments,
657 applications and resources. *Proceedings of the 2001 Congress on Evolutionary*
658 *Computation (IEEE Cat No01TH8546)* 1:81–86, DOI 10.1109/CEC.2001.934374,
659 URL [http://ieeexplore.ieee.org/lpdocs/epic03/wrapper.htm?arnumber=
660 934374](http://ieeexplore.ieee.org/lpdocs/epic03/wrapper.htm?arnumber=934374)<http://ieeexplore.ieee.org/xpls/abs/all.jsp?arnumber=934374>
- 661 Elkinton CN (2007) Offshore Wind Farm Layout Optimization. Doctor of philosophy
662 dissertation, University of Massachusetts Amherst
- 663 Elkinton CN, Manwell JF, McGowan JG (2008) Algorithms for offshore wind farm
664 layout optimization. *Wind Engineering* pp 67–83, URL <http://multi-science>.

-
- 665 metapress.com/index/Y14XL29NU6565RP1.pdf
- 666 Fagerfjäll P (2010) Optimizing wind farm layout - more bang for the buck using mixed
667 integer linear programming. Master of science dissertation, Chalmers University of
668 Technology and Gothenburgh University
- 669 Feng J, Shen WZ (2015) Solving the wind farm layout optimization problem using ran-
670 dom search algorithm. *Renewable Energy* 78:182–192, DOI 10.1016/j.renene.2015.01.
671 005, URL <http://dx.doi.org/10.1016/j.renene.2015.01.005>
- 672 Feng J, Shen WZ, Xu C (2016) Multi-Objective Random Search Algorithm for Si-
673 multaneously Optimizing Wind Farm Layout and Number of Turbines. *Journal of*
674 *Physics: Conference Series* 753(3):032,011, DOI 10.1088/1742-6596/753/3/032011
- 675 Gaillard H (2015) Optimization of export electrical infrastructure in offshore wind-
676 farms. Master of science thesis, KTH Industrial Engineering and Management
- 677 Gaumond M, Rethore P, Bechmann A (2012) Benchmarking of Wind
678 Turbine Wake Models in Large Offshore Windfarms. *Proceedings of*
679 *the Science of Making Torque from Wind Conference* Oldenburg, Ger-
680 many URL [http://www.eera-dtoc.eu/wp-content/uploads/files/](http://www.eera-dtoc.eu/wp-content/uploads/files/Gaumond-et-al-Benchmarking-of-wind-turbine-wake-models-in-large-offshore-wind-farms.pdf)
681 [Gaumond-et-al-Benchmarking-of-wind-turbine-wake-models-in-large-offshore-wind-farms.](http://www.eera-dtoc.eu/wp-content/uploads/files/Gaumond-et-al-Benchmarking-of-wind-turbine-wake-models-in-large-offshore-wind-farms.pdf)
682 [pdf](http://www.eera-dtoc.eu/wp-content/uploads/files/Gaumond-et-al-Benchmarking-of-wind-turbine-wake-models-in-large-offshore-wind-farms.pdf)
- 683 Gaumond M, Réthoré P, Ott S, Bechmann A, Hansen K (2013) Evaluation of the
684 wind direction uncertainty and its impact on wake modeling at the Horns Rev
685 offshore wind farm. *Wind Energy* DOI 10.1002/we, URL [http://onlinelibrary.](http://onlinelibrary.wiley.com/doi/10.1002/we.1625/full)
686 [wiley.com/doi/10.1002/we.1625/full](http://onlinelibrary.wiley.com/doi/10.1002/we.1625/full)
- 687 Geem ZW, Hong J (2013) Improved Formulation for the Optimization of Wind Tur-
688 bine Placement in a Wind Farm. *Mathematical Problems in Engineering* 2013(1):1–
689 5, DOI 10.1155/2013/481364, URL [http://www.hindawi.com/journals/mpe/2013/](http://www.hindawi.com/journals/mpe/2013/481364/)
690 [481364/](http://www.hindawi.com/journals/mpe/2013/481364/)
- 691 Grady S, Hussaini M, Abdullah M (2005) Placement of wind turbines using genetic al-
692 gorithms. *Renewable Energy* 30(2):259–270, DOI 10.1016/j.renene.2004.05.007, URL
693 <http://linkinghub.elsevier.com/retrieve/pii/S0960148104001867>

-
- 694 Gurobi Optimization Inc (2015) Gurobi Optimizer Reference Manual. URL [http://](http://www.gurobi.com)
695 www.gurobi.com
- 696 Hassan R, Cohanin B, de Weck O (2005) A comparison of particle swarm optimization
697 and the genetic algorithm. 1st AIAA multidisciplinary design optimization special-
698 ist conference pp 1–13, DOI 10.2514/6.2005-1897, URL [http://arc.aiaa.org/doi/](http://arc.aiaa.org/doi/pdf/10.2514/6.2005-1897)
699 [pdf/10.2514/6.2005-1897](http://arc.aiaa.org/doi/pdf/10.2514/6.2005-1897)
- 700 Hou P, Hu W, Soltani M, Chen C, Chen Z (2017) Combined optimization for offshore
701 wind turbine micro siting. *Applied Energy* 189:271–282, DOI 10.1016/j.apenergy.
702 2016.11.083, URL <http://dx.doi.org/10.1016/j.apenergy.2016.11.083>
- 703 Huang HS (2009) Efficient hybrid distributed genetic algorithms for wind turbine posi-
704 tioning in large wind farms. *IEEE International Symposium on Industrial Electron-*
705 *ics (ISIE):2196–2201*, URL [http://ieeexplore.ieee.org/xpls/abs/_all.jsp?](http://ieeexplore.ieee.org/xpls/abs/_all.jsp?arnumber=5213603)
706 [arnumber=5213603](http://ieeexplore.ieee.org/xpls/abs/_all.jsp?arnumber=5213603)
- 707 IEC (2006a) IEC 60228: Conductors of insulated cables, 3rd edn. International Elec-
708 trotechnical Commission, Geneva, Switzerland
- 709 IEC (2006b) IEC 60287: Electric Cables - Calculation of the current rating - Part 1-1:
710 Current rating equations (100% load factor) and calculation of losses - General, 2nd
711 edn. International Electrotechnical Commission, Geneva, Switzerland
- 712 Ituarte-Villarreal CM, Espiritu JF (2011) Optimization of wind turbine placement
713 using a viral based optimization algorithm. *Procedia Computer Science* 6:469–
714 474, DOI 10.1016/j.procs.2011.08.087, URL [http://linkinghub.elsevier.com/](http://linkinghub.elsevier.com/retrieve/pii/S1877050911005527)
715 [retrieve/pii/S1877050911005527](http://linkinghub.elsevier.com/retrieve/pii/S1877050911005527)
- 716 Kennedy J, Eberhart R (1995) Particle swarm optimization. *IEEE International*
717 *Conference on Neural Networks, 1995 Perth, Australia* 4:1942–1948 vol.4, DOI
718 10.1109/ICNN.1995.488968
- 719 Larsen GC (1988) A Simple Wake Calculation Procedure. Tech. rep., Risø National
720 Laboratory
- 721 Lindahl M, Bagger NF, Stidsen T, Ahrenfeldt SF, Arana I (2013) OptiArray from
722 DONG Energy. *Proceedings of the 12th Wind Integration Workshop (International*

-
- 723 Workshop on Large-Scale Integration of Wind Power into Power Systems as well as
724 on Transmission Networks for Offshore Wind Power Plants) London, UK
- 725 Makridis A, Chick J (2013) Journal of Wind Engineering Validation of a CFD model
726 of wind turbine wakes with terrain effects. *Jnl of Wind Engineering and Industrial*
727 *Aerodynamics* 123:12–29, DOI 10.1016/j.jweia.2013.08.009, URL [http://dx.doi.](http://dx.doi.org/10.1016/j.jweia.2013.08.009)
728 [org/10.1016/j.jweia.2013.08.009](http://dx.doi.org/10.1016/j.jweia.2013.08.009)
- 729 Marmidis G, Lazarou S, Pyrgioti E (2008) Optimal placement of wind turbines in a
730 wind park using Monte Carlo simulation. *Renewable Energy* 33(7):1455–1460, DOI
731 10.1016/j.renene.2007.09.004, URL [http://linkinghub.elsevier.com/retrieve/](http://linkinghub.elsevier.com/retrieve/pii/S0960148107002807)
732 [pii/S0960148107002807](http://linkinghub.elsevier.com/retrieve/pii/S0960148107002807)
- 733 Mittal A (2010) Optimization of the Layout of Large Wind Farms Using a Genetic
734 Algorithm. Master of science dissertation, Case Western Reserve University
- 735 Mosetti G, Poloni C, Diviacco B (1994) Optimization of wind turbine positioning
736 in large wind-farms by means of a genetic algorithm. *Journal of Wind Engineering*
737 *and Industrial Aerodynamics* 51(1):105–116, URL [http://www.sciencedirect.com/](http://www.sciencedirect.com/science/article/pii/0167610594900809)
738 [science/article/pii/0167610594900809](http://www.sciencedirect.com/science/article/pii/0167610594900809)
- 739 NOREL Group (2014) Nautical and Offshore Renewable Energy Liaison Group
740 (NOREL) Minutes of the 29th NOREL held on 8 May 2014. Tech. Rep. May, The
741 Crown Estate
- 742 Pillai A, Chick J, Johanning L, Khorasanchi M, Pelissier S (2016a) Optimisation of
743 Offshore Wind Farms Using a Genetic Algorithm. *International Journal of Offshore*
744 *and Polar Engineering* 26(3):225–234, DOI 10.17736/ijope.2016.mmr16
- 745 Pillai AC, Chick J, de Laleu V (2014) Modelling Wind Turbine Wakes at Middelgrun-
746 den Wind Farm. In: *Proceedings of European Wind Energy Conference & Exhibition*
747 *2014 Barcelona, Spain*, pp 1–10
- 748 Pillai AC, Chick J, Johanning L, Khorasanchi M, Barbouchi S (2016b) Comparison of
749 Offshore Wind Farm Layout Optimizaiton Using a Genetic Algorithm and a Particle
750 Swarm Optimizer. In: *Proceedings of the ASME 2016 35th International Conference*
751 *on Ocean, Offshore and Arctic Engineering (OMAE 2016) Busan, South Korea,*

-
- 752 ASME, vol 6, pp 1–11, DOI 10.1115/OMAE2016-54145
- 753 Pillai ACAAC, Chick J, Johanning L, Khorasanchi M, de Laleu V (2015)
754 Offshore wind farm electrical cable layout optimization. Engineering Op-
755 timization 47(12):1689–1708, DOI 10.1080/0305215X.2014.992892, URL
756 <http://www.tandfonline.com/doi/abs/10.1080/0305215X.2014.992892>
757 [http://www.scopus.com/inward/record.url?eid=2-s2.0-84922374336&partnerID=](http://www.scopus.com/inward/record.url?eid=2-s2.0-84922374336&partnerID=tZ0tx3y1)
758 [tZ0tx3y1](http://www.scopus.com/inward/record.url?eid=2-s2.0-84922374336&partnerID=tZ0tx3y1)
- 759 Pookpant S, Ongsakul W (2013) Optimal placement of wind turbines within wind
760 farm using binary particle swarm optimization with time-varying acceleration co-
761 efficients. Renewable Energy 55:266–276, DOI 10.1016/j.renene.2012.12.005, URL
762 <http://linkinghub.elsevier.com/retrieve/pii/S0960148112007604>
- 763 Renkema DJ (2007) Validation of wind turbine wake models. Master of science disser-
764 tation, TU Delft
- 765 Réthoré PE, Fuglsang P, Larsen TJ, Buhl T, Larsen GC (2011) TOPFARM wind farm
766 optimization tool. Riso DTU National Laboratory for Sustainable Energy
- 767 Rodrigues S, Restrepo C, Katsouris G, Teixeira Pinto R, Soleimanzadeh M, Bosman P,
768 Bauer P (2016) A Multi-Objective Optimizaiton Framework for Offshore Wind Farm
769 Layouts and Electric Infrastructures. Energies 9(3):1–42, DOI 10.3390/en9030216
- 770 Shakoor R, Yusri M, Raheem A, Rasheed N (2016) Wind farm layout optimization
771 using area dimensions and definite point selection techniques. Renewable Energy
772 88:154–163, DOI 10.1016/j.renene.2015.11.021, URL [http://dx.doi.org/10.1016/](http://dx.doi.org/10.1016/j.renene.2015.11.021)
773 [j.renene.2015.11.021](http://dx.doi.org/10.1016/j.renene.2015.11.021)
- 774 Tegen S, Hand M, Maples B, Lantz E, Schwabe P, Smith A (2012) 2010 Cost of Wind
775 Energy Review. Tech. Rep. April, National Renewable Energy Laboratory (NREL)
- 776 Tegen S, Lantz E, Hand M, Maples B, Smith A, Schwabe P (2013) 2011 Cost of Wind
777 Energy Review. Tech. Rep. March, National Renewable Energy Laboratory
- 778 Thøgersen ML (2005) WindPRO / PARK. EMD International A/S, URL www.emd.dk
- 779 Van Den Bergh F, Engelbrecht AP (2006) A study of particle swarm optimization
780 particle trajectories. Information Sciences 176(8):937–971, DOI 10.1016/j.ins.2005.

781 02.003

782 Wan C, Wang J, Yang G, Zhang X (2010a) Optimal Micro-siting of Wind Farms by
783 Particle Swarm Optimization. Lecture Notes in Computer Science2 DOI 10.1007/
784 978-3-642-13495-1_25

785 Wan C, Wang J, Yang G, Zhang X (2010b) Particle swarm optimization based on
786 Gaussian mutation and its application to wind farm micro-siting. 49th IEEE Con-
787 ference on Decision and Control (CDC) (July 2015):2227–2232, DOI 10.1109/CDC.
788 2010.5716941

789 Zhang PY (2013) Topics in Wind Farm Layout Optimisation: Analytical Wake Models,
790 Noise Propagation, and Energy Production. Master of applied science dissertation,
791 University of Toronto

792 Zhang PY, Romero DA, Beck JC, Amon CH (2014) Solving wind farm layout opti-
793 mization with mixed integer programs and constraint programs. EURO Journal on
794 Computational Optimization 2(3):195–219, DOI 10.1007/s13675-014-0024-5, URL
795 <http://link.springer.com/10.1007/s13675-014-0024-5>